doi:10.3788/gzxb20124104.0394

Electro-optic Effect of Glass Waveguides with Lower Threshold of Poling Conditions

ZHANG Li-ping

(*College of Medical Technology, Qiqihar Medical University, Qiqihar, Heilongjiang* 161006, *China*)

Abstract: Silicon-based channel waveguides are poled by thermal poling. A fiber-based (single mode) Mach- Zehnder interferometer is utilized to measure the linear electro-optic effect. Poling conditions (poling temperature, poling time, poling voltage) are optimized in air environment. The results show that, the electro-optic coefficient is $r_{TM}=0.059\pm0.001$ pm/V, $r_{TE}=0.053\pm0.001$ pm/V at the optimized conditions (−2.4 kV, 406℃, 20 min). At the same time, the waveguide has a lower threshold of poling voltage and poling temperature. An effective electro-optic signal can be observed when poling voltage drops to about 100 V or poling temperature drops to about 80℃. The results also suggest that the electro-optic coefficient increases of 15% at negative poling than positive poling.

Key words: Channel waveguides; Thermal poling; Electro-optic effect; Optical waveguide; Glass

CLCN: TN256 **Document Code**: A **Article ID**: 1004-4213(2012)04-0394-5

0 Introduction

Glass is the most important material in optical communication and optical integration because of low manufacture cost, stable physical properties, and good compatibility with optical fibers. However, glass is a kind of amorphous materials, which prevents it from showing second-order nonlinear effect, and limits its applications in optical communication. In 1991, Myers *et. al.*[1] found that a large second nonlinearity could be induced in fused silica by thermal poling technology. Since then, nonlinear optical effect from poled glass has been widely researched by various methods, e. g. thermal poling[1-3], optical poling[4-5], and UV[6-7] poling. Primary research work has been spent on the poling of bulk silica[8-10] and silica fibers[11-13] compared to the poling of glass waveguides. Because silica-based waveguides are the foundation of future optical integration, it is a very important research work about poled of silica-based waveguides. Meanwhile, silica-based waveguides also provide potential applications in producing electro-optic modulator, optical frequency mixer, optical switching, and wavelength converters.

1 Experimental procedure

1.1 Sample preparation

Waveguide samples with four-layer structure were manufactured on silicon wafers. The lower and upper cladding layers of pure SiO_2 were grown by thermal oxidation and plasma enhanced chemical vapor deposition (PECVD) grown on silicon wafers. The core layer by PECVD consisted of germanium-doped silicon oxynitride (Ge: SiON). A thin silicon oxynitride layer (SiON) was added on core layer, that the added layer served as charge-trapping layer to increase the density of the charge deposited on the top of the core layer, as shown in Fig. 1. Waveguide channels (4 to 10 μm in width) were formed in the core layer under ultraviolet radiation (KrF excimer laser, 248 nm)

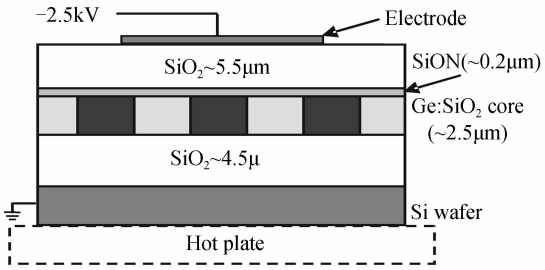

Fig. 1 The channel waveguides structure and a schematic drawing of the poling process

Foundation item: The National Natural Science Foundation of China (No. 60867002) and the Science and Technology Bureau Foundation of Qiqihar

Author: ZHANG Li-ping (1978−), male, lecturer, M. S. degree, mainly focuses on optoelectronic and optical waveguide device. Email: zhangliping@qqhrmu.cn

Received date: 2011-10-18 **Revised date**: 2011-12-20

through an aluminum mask after a high pressure deuterium loading[14].

Silver paint electrode was put on the top of the cleaved waveguide chips. The waveguides were poled at a large static electric field at elevated temperature in air on an open hotplate. High DC voltage (negative bias) was applied across the samples via electrodes for poling while the silicon wafer was kept grounded. The poling time was started from the voltage turned on at the poling temperature and was stopped until the heating stage was turned off, while the voltage was maintained until room temperature arrives.

1.2 Electro-optic effect measurement

A fiber-based (single mode) Mach-Zehnder interferometer was utilized to measure induced nonlinear effect or linear electro-optic (LEO) coefficients about the poled waveguide samples as shown in Fig. 2.

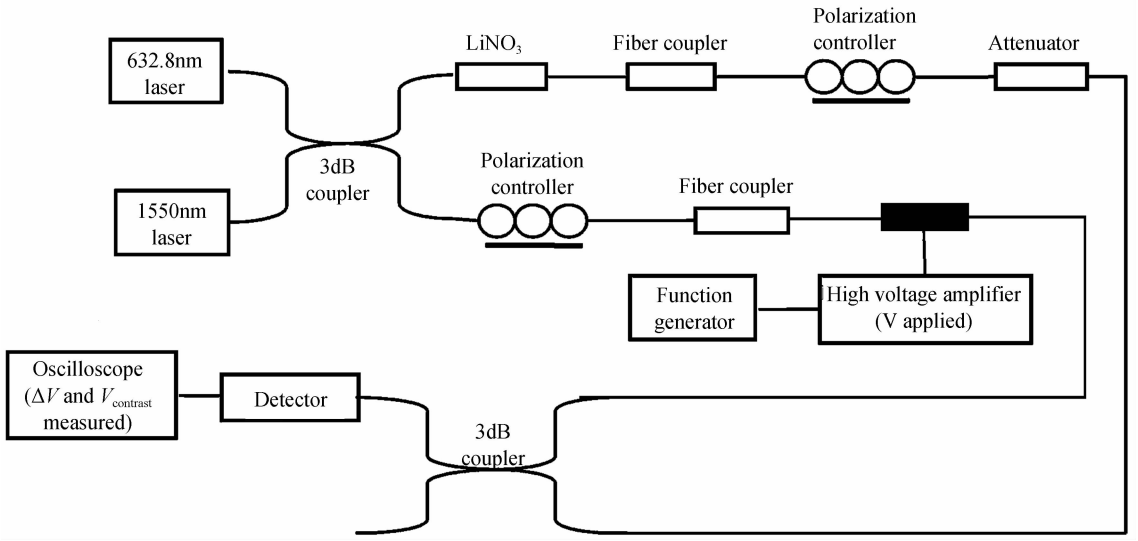

Fig. 2　Electro-optic effect measurement system based on a Mach-Zehnder interferometer

Laser light (1 550 nm) from a semiconductor laser was divided into two equal beams (measurement arm and reference arm) via a 3-dB coupler. Modulated signal from the sample in the measurement arm was then coupled with the reference signal by another 3-dB coupler leading to a detector with frequency filter. A commercial $LiNbO_3$ phase modulator was employed in the reference arm to calibrate the phase shifts induced from the poled channel waveguides. The desired polarization states into the samples were controlled to the direction parallel (*p*-component input) or perpendicular (*s*-component input) to that of the applied testing field. The interference fringes with the highest contrast were achieved by balancing the intensity and matching the polarization states in both arms. A permanent EO effect was observed in all samples after poling. The LEO coefficients are given in equation below by measuring the phase shift (compared with a reference phase shift from $LiNbO_3$ phase modulator) from the poled waveguide samples.

$$r=\frac{\lambda d}{\pi V L n^3}\Delta\varphi \tag{1}$$

where $\Delta\varphi = 2\arcsin(\Delta V/V_{\text{constrast}})$ is the induced phase shift of the poled waveguides; V_{contrast}, as shown in Fig. 3(a), is the maximum signal (peak-to-peak) induced from the $LiNbO_3$ phase modulator when half wave voltage was applied to

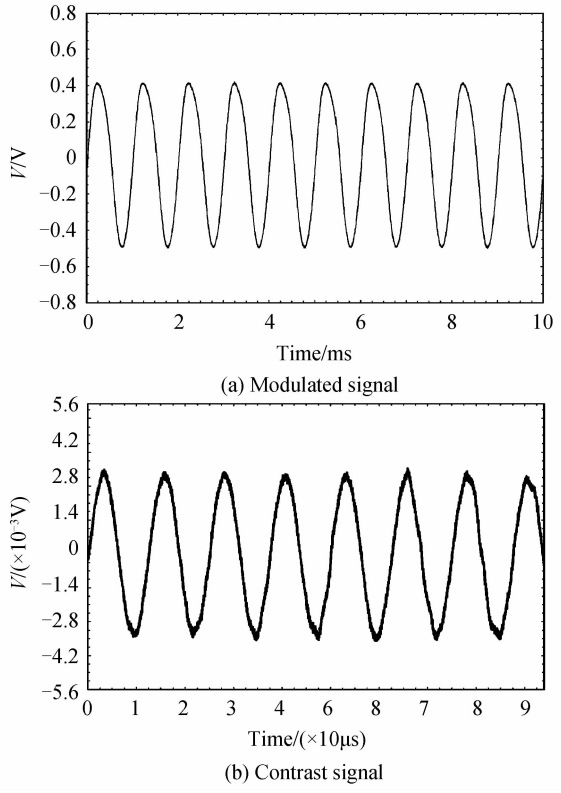

Fig. 3　Modulated and contrast signals

$LiNbO_3$ phase modulator; and ΔV, as shown in Fig. 3(b), is the modulated signal (peak-to-peak) induced from the poled waveguide samples under the same frequency when the testing voltage was applied to poled waveguides. $V_{contrast}$ and ΔV were measured from oscilloscope. λ (1 550 nm) is the wavelength, d is the thickness of the samples, V which was from high voltage amplifier and function generator is the testing voltage (peak-to-peak) that was applied to waveguides (110 V), L is the length of the top electrode, and n is the refractive index of the core layer [14].

2 Results and discussion

The influence of poling conditions (poling temperature, time and voltage) on the EO coefficient was systematically studied. The corresponding results are shown in Fig. 4～6.

2.1 Dependence of EO coefficients on poling temperature

Fig. 4 shows the dependence of EO coefficients on the poling temperature after the samples were poled with −2.0 kV for 20 min.

Temperature studies clearly show that an threshold temperature (80℃) was lower than the report of silica glass (150℃) [15] as shown in Fig. 4(a). When the temperature was lower than the threshold temperature, the applied poling voltage (−2.0 kV) didn't overcome the net restraint and produce nonlinear optical effect in the waveguides. Experiments also found that it was intermittent and extremely unstable singals when poling temperature arrived at 100℃. As poling temperature was further increased, the net restraint was rapidly reduced thus favoring the charges moving or dipole/bond alignment and an increase in EO coefficients. When temperature was optimal poling temperature (406℃) as shown in Fig. 4(b), the restraint became very small and the charges or dipoles could move almost freely, a maximum EO signals was reached at the balance of the poling field and thermal relaxation. When the temperature was higher than the optimal poling temperature, the strong thermal motion would randomize the charges or dipoles motion thus reduing the EO coefficients.

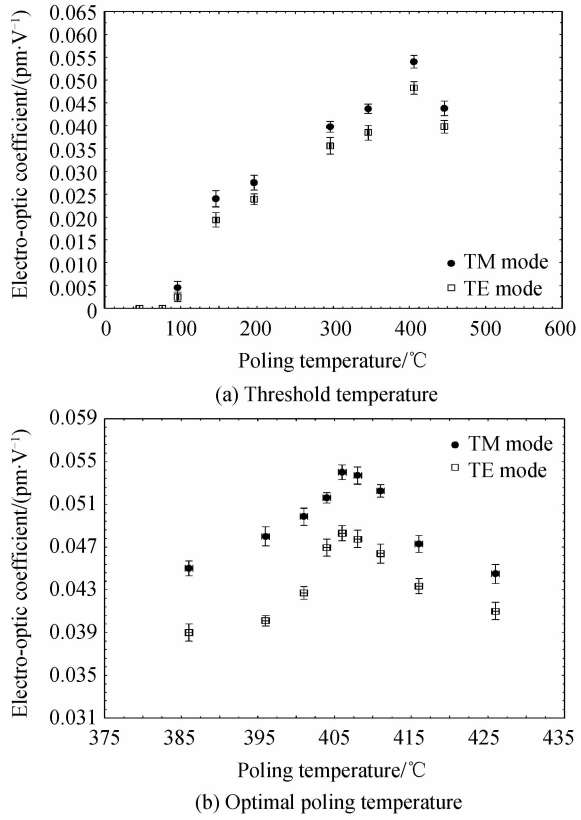

Fig. 4 Changes of EO coefficients with poling temperature (poled at −2.0 kV for 20 min)

2.2 Dependence of EO coefficients on poling time

Fig. 5 shows the dependence of EO coefficients on the poling time after the samples were poled with − 2.0 kV and the optimum poling temperature (406℃) for variable time.

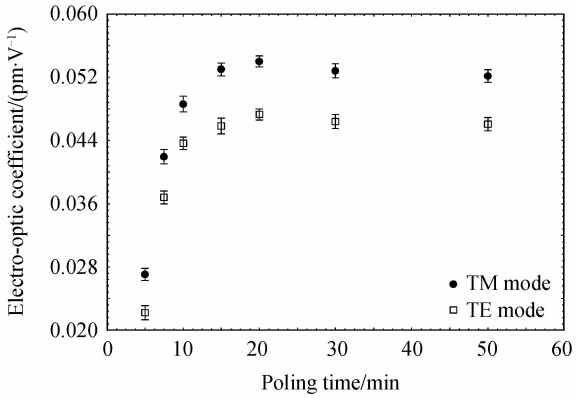

Fig. 5 Changes of EO coefficients with poling time (poled at −2.0 kV and 406 ℃)

The obtained results demonstrate that the nonlinear effect was built up quickly in the sample during the initial poling stage and approached a saturation at 30 min, which is shorter than the report of silica glass (3 h)[15]. Small changes of the EO coefficients were observed when poling between 10 and 50 min. The EO coefficients decrease lightly when poling for a prolonged time. The reason was that the width of depletion region could be written as $L \propto \ln(t)$[16], where L is the width of depletion region and t is the poling time. If extended the poling time, the depletion region will move deeply inside the sample. This may leads to a poor spatial overlap between the depletion region and the core layer of sample.

2.3 Dependence of EO coefficients on poling voltage

Fig. 6 shows the dependence of EO coefficients on the poling voltage after the samples were poled with the optimum poling temperature (406℃) and optimum time (20 min) for variable voltage.

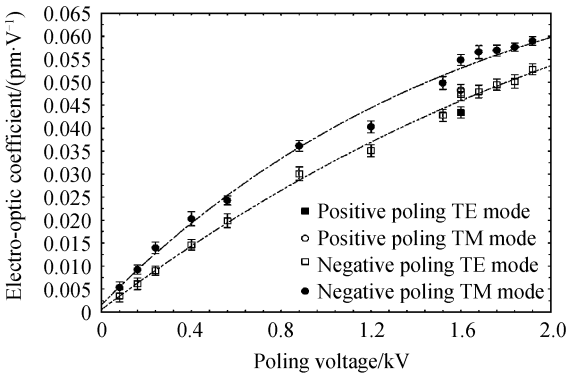

Fig. 6　Changes of EO coefficients with poling voltage (poled at 406 ℃ for 20 min)

The obtained results demonstrate that a lower threshold voltage was existence (100 V). Currently, we have not seen the reports about such low threshold voltage, which is more lower than silica glass[17]. This provides an important experimental basis for achieving nonlinear effect at lower poling voltage. When the poling voltage was lower than threshold voltage, the nonlinear effects were not produced and charges or dipoles were random thermal motion. It is a quasi-linear relationship between EO coefficients and poling voltage, when poling voltage was higher than threshold voltage. It is a better linear relationship at the lower voltage than the higher voltage. Increasing of the EO coefficients was slower at the higher voltage because of the limited numbers of charges or dipoles available in the waveguides. Figs. 6 also shows the EO coefficient of the waveguides with negative poling is ($r_{TM}=0.059\pm0.001$, $r_{TE}=0.053\pm0.001$) pm/V, corresponding to ($\chi^{(2)}=0.015\pm0.002$) pm/V, which is about 15% greater than that with positive poling. It also provides an effective way for increasing the nonlinear effect of silica glass.

3 Conclusion

Channel waveguides with a thin silicon oxynitride layer were poled by negative high DC voltage. Poling conditions (poling temperature, poling time and poling voltage) were optimized by systematical investigations in air environment. It is found that the waveguide has a lower threshold of poling voltage (100 V) and poling temperature (80℃) at the optimized poling time, which is much lower than silica glass. The experimental results suggest that the electro-optic coefficient increases about 15% at negative poling than positive poling. It also provides some effective ways for increasing the nonlinear effect of silica glass, for example, improving poling voltage (vaccum poling), changing the polarity of poling voltage (negative poling) and changing waveguide structure (charge-trapping layer).

References

[1] MYERS R A, MUKHERJEE N, BRUECK S R J. Large second-order nonlinearity in poled fused silica[J]. *Optics Letters*, 1991, **16**(22): 1732-1734.

[2] FLEMING S, AN H. Progress in creating second-order optical nonlinearity in silicate glasses and waveguides through thermal poling[J]. *Fronierst Optoelectronics in China*, 2010, **3**(1): 84-91.

[3] MARIAPPAN C R, ROLING B. Mechanism and kinetics of Na^+ ion depletion under the anode during electro-thermal poling of a bioactive glass[J]. *Journal of Non-crystalline Solids*, 2010, **356**(11-17): 720-724.

[4] OSTERBERG U, MARGULIS W. Dye laser pumped by Nd: YAG laser pulses frequency in a glass optical fiber[J]. *Optics Letters*, 1986, **11**(8): 516-518.

[5] SOULIS M, DUCLèRE J R, COUDERC V, *et al*. Second Harmonic Generation induced by optical poling in new TeO_2-Tl_2O-ZnO glasses[J]. *Materials Research Bulleti*, 2010, **45**(5): 551-557.

[6] FUJIWARA T, WONG D, ZHAO Y, *et al*. Electro-optic modulation in germanosilicate fiber with UV-excited poling [J]. *Electronics Letters*, 1995, **31**(7): 573-575.

[7] FUJIWARA T, TAKAHASHI M, IKUSHIMA A J. Second-harmonic generation in germanosilicate glass poled with ArF laser irradiation[J]. *Applied physics Letters*, 1997, **71**(8): 1032-1034.

[8] MOURA A L, NASCIMENTO E M, ARAUJO M T, *et al*. Voltage thresholdlike evidence during thermal-electric field induction of second order nonlinearity in soda-lime glassed[J]. *Journal of Applied Physics*, 2009, **105**(3): 036106.

[9] QIU M X, VILASECA R, COJOCARU C, *et al*. Second-order optical nonlinearity generated by doping the surface layer of silica with anions or cations[J]. *Journal of Applied Physics*, 2000, **88**(8): 4666-4670.

[10] MATSUMOTO S, FUJIWARA T, IKUSHIMA A J. Large second-order optical nonlinearity in Ge-doped silica glass[J]. *Optical Materials*, 2001, **18**(1): 19-22.

[11] WONG D, XU W, JANOS M, *et al*. Time evolution of electro-optic effect in fiber during thermal poling[J]. *Japanese Journal Applied Physics*, 1998, **37**(1): 68-70.

[12] KAZANSKY P G, RUSSELL P S J, TAKEBE H. Glass fiber poling and applications[J]. *Journal of Lightwave Technology*, 1997, **15**(8): 1484-1493.

[13] WONG D, XU W, FLEMING S, *et al*. Frozen-in electrical field in thermally poled fibers[J]. *Optical Fiber Technology*, 1999, **5**(2): 235-241.

[14] REN Y T. Nonlinear effect induced in thermally poled glass waveguides[J]. *Journal of Zhejiang University Science A*, 2006, **7**(1): 105-108.

[15] XU J H, LU X Z, CHEN H B, *et al*. Second harmonic generation investigation on electric poling effects in fused silica[J]. *Optical Materials*, 1997, **8**(4): 243-247.

[16] ALLEY T G, BRUECK S R J. Visualization of the nonlinear optical space-charge region of bulk thermally poled fused-silica glass[J]. *Optics Letters*, 1998, **23**(15): 1170-1172.
[17] QUIQUEMPOIS Y, GODBOUT N, LACROIX S. Modal of charge migration during thermal poling in silica glasses: Evidence of a voltage threshold for the onset of a second-order nonlinearity[J]. *Physical Review A*, 2002, **65**(4): 043816.

低阈值极化电压玻璃光波导电光效应的研究

张立平
(齐齐哈尔医学院 医学技术学院, 黑龙江 齐齐哈尔 161006)

摘 要:采用热极化技术对掺锗玻璃条形光波导进行极化,通过光纤连接(单模)的 Mach Zehnder Interferometer 系统测量条形波导内诱导出的电光效应,系统地研究了大气环境下极化条件(极化温度、极化时间、极化电压)对电光效应的影响.结果表明:在最佳极化条件下(406℃、−2.4 kV、20 min),波导内的电光系数为 $r_{TM}=0.059\pm0.001$ pm/V, $r_{TE}=0.053\pm0.001$ pm/V,且波导结构中存在一个较低的阈值极化电压(100 V)和阈值极化温度(80℃),此时在波导样品内仍能被激发出可观察的电光效应;实验还发现采用负极化诱导方式产生的电光系数较正极化提高15%左右.

关键词:条形波导;热极化;电光效应;光波导;玻璃